Separation Science and Technology
Publication details, including instructions for authors and subscription information:
http://www.informaworld.com/smpp/title~content=t713708471

A New Continuous Flow Reactor for Simultaneous Reaction and Separation

B. K. Cho[a]; R. W. Carr[a]; R. Aris[a]
[a] Department of Chemical Engineering and Materials Science, Minnesota

To cite this Article Cho, B. K. , Carr, R. W. and Aris, R.(1980) 'A New Continuous Flow Reactor for Simultaneous Reaction and Separation', Separation Science and Technology, 15: 3, 679 — 696
To link to this Article: DOI: 10.1080/01496398008068503
URL: http://dx.doi.org/10.1080/01496398008068503

SEPARATION SCIENCE AND TECHNOLOGY, 15(3), pp. 679-696, 1980

A NEW CONTINUOUS FLOW REACTOR FOR SIMULTANEOUS REACTION AND SEPARATION

B. K. Cho, R. W. Carr and R. Aris
Department of Chemical Engineering and Materials Science
421 Washington Avenue S.E.
Minneapolis, Minnesota 55455

ABSTRACT

The acid catalysed hydrolysis of methylformate has been investigated in a continuous flow annular reactor packed with activated charcoal, and equipped with a rotating feed injection port. Chromatographic separation of the products, formic acid and methanol, effectively suppressed the reverse reaction, causing conversions to be significantly greater than the thermodynamic equilibrium conversions that would have been obtained in the absence of separation. Comparisons of numerically simulated reactor performance with experimental results showed good agreement, although some differences occurred as experimentation proceeded, most probably due to deactivation of the activated charcoal.

INTRODUCTION

It is well known that the chromatographic separation in reaction chromatography can enhance the net forward progress of reaction when the chemical reaction is of the type

$$aA \rightleftharpoons bB + cC + \cdots .$$

Chromatographic reactors have usually consisted of a packed column containing a combined catalyst-solid adsorbent, with the reactant being injected as a pulse into a continuously flowing carrier fluid (1-10).

Martin (11) appears to have first suggested the possibility that continuous chromatography could be done in the packed annular space between the walls of two concentric cylinders by rotating the assembly. Giddings (12) later discussed the feasibility of a continuous chromatographic system of this type. Recently, it was demonstrated experimentally that chromatography can be done on a continuous basis in a number of different configurations. A rotating annular chromatograph (13-15); spaced, rotating discs (16); a rectangular slab (17); and countercurrent chromatography (18) have all been used successfully. Recently, Viswanathan and Aris (19) explored the combination of continuous chromatography and reaction chromatography in a countercurrent moving bed reactor for an irreversible reaction of the Type $A \rightarrow B$.

Most studies with the pulsed chromatographic reactor were concerned with quick estimation of kinetic parameters rather than with chemical reactor development. To develop reaction chromatography toward practical applications, continuous operation would be most desirable.

In this paper we report the combination of reaction chromatography with continuous chromatography in a rotating annular type of a chromatographic reactor. For reactions of the type $aA \rightleftharpoons bB + cC$, separation of the products will suppress the backward reaction and may lead to enhanced yields. This would be of advantage in cases where thermodynamic equilibrium is unfavorable. The reactor is a stationary, packed cylindrical annulus with a rotating feed port. A study of the acid catalyzed hydrolysis of methylformate

$$\underset{(A)}{HCOOCH_3} + H_2O \overset{H^+}{\rightleftharpoons} \underset{(B)}{CH_3OH} + \underset{(C)}{HCOOH} \qquad (1)$$

was conducted using dilute hydrochloric acid as the catalyst and carrier fluid. Also, a mathematical model was used to numerically simulate reactor performance.

EXPERIMENTAL

Reactor

A cross-sectional view of the Plexiglas reactor is shown in Fig. 1. Since the feed port rotates and the annulus is stationary, the eluent concentration "peaks" travel around the annular outlet, lagging the feed port position by a distance that is primarily a function of their retention by the stationary phase. Details of construction and experimental procedures are given in ref. (20).

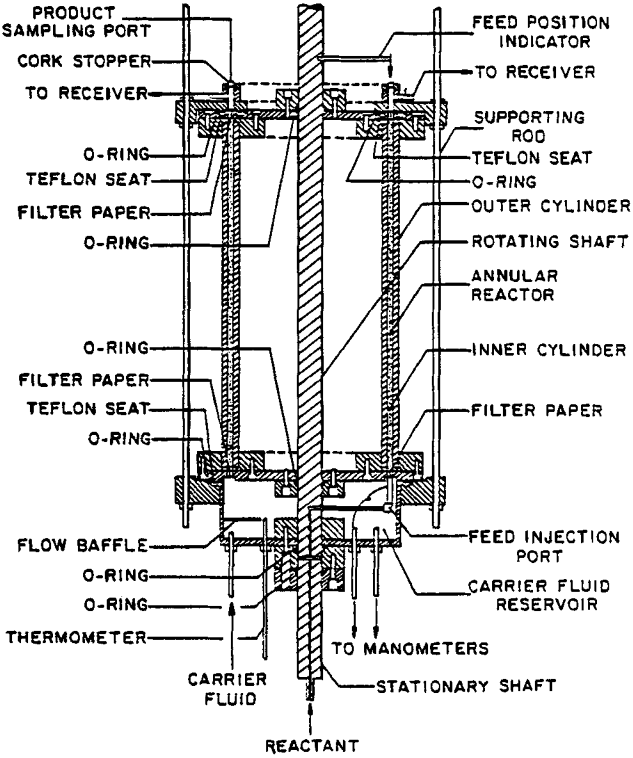

Figure 1 The reactor assembly.

Preliminary Experiments

Adsorption experiments were carried out using a commercial, 60-80 mesh, activated coconut charcoal, manufactured by Fisher Scientific Company, as the adsorbent. Single-solute isotherms were obtained for methanol-water, formic acid-water, methylformate-water, and methanol-1N hydrochloric acid systems by the static method (21). The experimental data shown in Fig. 2 gave good fits to Freundlich isotherms. The parameter values, obtained by the least squares method, for the Freundlich isotherm model

$$n_i = K_i c_i^{m_i} , \quad i = A, B, C \tag{2}$$

are

$$\begin{aligned} K_A &= 3.48 \times 10^{-3} \text{ mole/gr-adsorbent}, & m_A &= 0.33 \\ K_B &= 1.40 \times 10^{-3} \text{ mole/gr-adsorbent}, & m_B &= 0.72 \\ K_C &= 3.45 \times 10^{-3} \text{ mole/gr-adsorbent}, & m_C &= 0.26 \end{aligned} \tag{3}$$

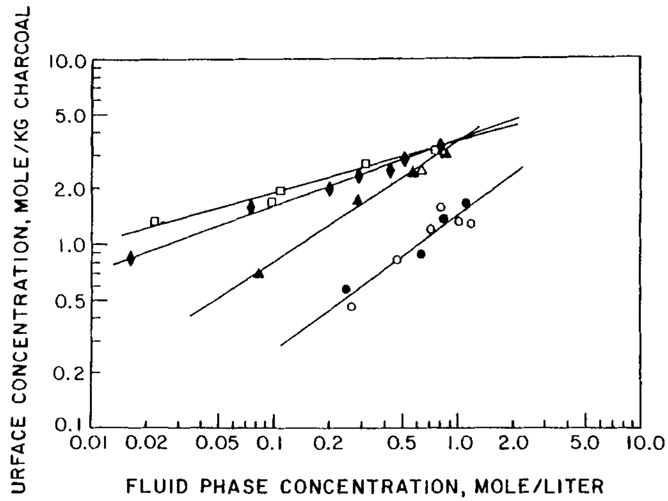

Figure 2 Single-solute adsorption isotherm on activated coconut charcoal. Fresh adsorbent; ♦ $HCOOCH_3$-H_2O, □ $HCOOH$-H_2O, ▲CH_3OH-H_2O, △ CH_3OH-1N HCl. Aged adsorbent; ○CH_3OH-H_2O, ● CH_3OH-1N HCl.

The presence of 1N hydrochloric acid proved to have negligible effect on the adsorption isotherms. It was observed that, after long use in the 1N HCl environment (approximately 100 hours), the adsorption capacity of charcoal for methanol decreased as evidenced in Fig. 2, possibly because of deactivation or impurity contamination. The above parameter values for methanol, K_B and m_B, are for the methanol adsorption on aged charcoal in 1N HCl.

Experimental data for multi-solute adsorption were fitted to the Langmuir isotherm, but reliable parameter values could not be obtained. This may be due partly to interactions between solutes in the fluid phase, possibly hydrogen bonding, and partly to the highly heterogeneous nature of the activated charcoal surface.

The same batch of adsorbent as used in the adsorption isotherm measurement was packed into the annular reactor space by a dry free-falling technique through a funnel rotating at 1 rpm. The bed packing density was determined to be 0.543 gr charcoal/cc of bed, and a void fraction of 0.54. The degree of uniformity in bed packing was checked by measuring the elution profile of a trace component (in this case methanol) at several different feed positions around the annular region, while keeping the feed port stationary. The shapes of concentration peaks coming from different feed positions were in reasonable agreement, indicating that while the packing is not strictly uniform, it is reasonably good.

The chemicals used were Eastman Kodak's Spectro grade methylformate, Fisher Scientific's Certified A.C.S. grade anhydrous methyl alcohol, Mallinckrodt's Analytical grade aqueous formic acid, Hi-Pure Chemicals' Electronic grade hydrochloric acid, and Chippews Springs' distilled water. Samples were analyzed by gas chromatography on a 6 mm O.D.×6 ft glass column packed with Porapak Q and operated at 130°C.

Procedures

Reactant and carrier fluid flow was driven by a pressurized system connected to compressed air cylinders. The range of flow rates of the carrier was 10-20 ml/min and that of the reactant was maintained at 3/97 of the carrier flow rate. Flow rates were measured by Fischer and Porter rotameters. The overall pressure drop through the system was ca. 300 mm Hg for the carrier flow and ca. 130 mm Hg for the reactant flow. The reactant feed port was rotated at 0.01-0.05 rad/min. The carrier fluid was fed along the whole annular area except the region where the reactant feed port was located. To minimize mixing between the carrier and the reactant before they entered the reactor bed, pressures at the reactant feed port and the carrier fluid reservoir were kept approximately the same. Product samples were taken from the fifty sampling positions provided around the annular area at the exit of the reactor, and two different sampling schemes were used. In one scheme, samples were taken at desired angular distances from the rotating feed port, which is essentially a sampling method in a moving coordinate system whose origin is fixed at the rotating feed port. In the other scheme, samples were taken at a fixed point, with the angular distance between the sampling point and the rotating feed port varying with time. Both sampling schemes should give the same elution profile if the reactor bed packing is everywhere uniform.

PREDICTION OF REACTOR PERFORMANCE

A mathematical model has been developed to predict the reactor performance. In describing our present reactor system mathematically, it is assumed that the reactor bed packing is uniform and can be treated as a homogeneous continuum. Since the adsorbent particle size is very small (60-80 mesh) and the fluid flow velocity is very slow (ca. 1.0 cm/min), adsorption equilibrium between the fluid and the solid phase can be assumed throughout the reactor, which operates isothermally. The width of the annular space is so thin compared to the radius of two concentric cylinders that $R_1 \doteq R_2 \doteq R$ can be assumed, where R_1 and R_2 are the radius of the inner and the outer cylinder, respectively. The distribution of fluid velocity and concentration is assumed to be uniform across the reactor bed. Since the fluid phase is liquid, it can be assumed that the effect of pressure drop along the reactor and dispersive effects in the fluid phase are negligible. Material balances for each component over the reactor give the following model equations:

$$\varepsilon u_z \frac{\partial c_i}{\partial z} + \omega \frac{\partial}{\partial \phi} \{\varepsilon c_i + \rho_B n_i\} = \alpha_i [H^+]\ k(c_A - c_B c_C / K_e) \qquad (i = A,\ B,\ C) \tag{4}$$

$$\alpha_i = \begin{cases} -1 & \text{for } i = A \\ 1 & \text{for } i = B,\ C \end{cases} \tag{5}$$

The inlet and boundary conditions are

$$c_i(0,\phi) = \begin{cases} c_{io} & \text{for } 0 \le \phi \le \Phi \\ 0 & \text{for } \Phi < \phi < 2\pi \end{cases} \tag{6}$$

$$c_i(z,0) = c_i(z,\ \phi + 2\pi) \tag{7}$$

In Eq. (4) the surface concentration n_i is related to the fluid phase concentration c_i through the Freundlich adsorption isotherm in Eq. (2), and $[H^+]$ represents the hydrogen ion concentration in mole/ℓ.

Eqs. (4) through Eq. (7) were solved using a finite difference scheme based upon Lax' method (22), the details of which will be reported elsewhere.

EXPERIMENTAL RESULTS

The upper limit of methylformate concentration in the feed stream was limited by the miscibility of methylformate with water, which is 30 gr/100 gr of H_2O at 20°C (23). Consequently, the methylformate concentration in the feed stream was kept below 3.0 mole/ℓ, which is well below the solubility limit. Although the reaction is slightly endothermic, with a heat of reaction of about 4.0 Kcal/mole (24), the rate of heat absorption was too small to disturb the temperature of the reactor bed.

A virtual steady state was reached after one complete revolution of the reactor, which corresponds to about seven hours of operation with $\omega = 0.15$ rad/min. For one experimental run, it took approximately 24-30 hours of continuous operation.

It has already been noted that the bed packing was not perfectly uniform. As a result, the elution profile obtained by the rotating sampling scheme gave more scatter than the fixed-point sampling scheme. Except where indicated, the fixed-point sampling scheme was used. The product samples were taken through sampling holes at the top of the reactor using a 10 $\mu\ell$ Hamilton microsyringe. After an experimental run was completed, the reactor bed was washed out with distilled water until no residual solute peak was detected in the effluent stream.

The experimental conditions are given in Table 1. In the numerical simulation, literature values of the reaction rate constant and the reaction equilibrium constant (25)

TABLE 1. Experimental Conditions

Figure	3	4	5	6	7	8	9
Temp., °C	26±1	25±1	25±1	25±1	25±1	25±1	25±1
u_z, cm/min	1.04	1.04	1.04	1.04	1.04	1.04	0.52
ω, rad/min	0.032	0.032	0.0151	0.0151	0.0151	0.0151	0.0151
Pressure, mm Hg							
(Carrier feed tank)	310	310	310	310	310	310	310
(Reactor feed tank)	127	125	127	127	127	127	127
Feed condition							
(c_{A0}, mole/ℓ)	3.0	0.32	3.0	3.0	2.0	1.5	3.0
(c_{B0}, mole/ℓ)	0	2.33	0	0	0	0	0
(c_{C0}, mole/ℓ)	0	1.56	0	0	0	0	0
Carrier fluid	1N-HCl	1N-HCl	1N-HCl	0.5N-HCl	1N-HCl	1N-HCl	1N-HCl
Flow rate, cc/min							
(Carrier)	20	20	20	20	20	20	20
(Reactant)	0.62	0.62	0.62	0.62	0.62	0.62	0.62
Sampling method	F*	R**	F	F	F	F	F

*F = fixed-point sampling, **R = rotating sampling.

$k = 0.176\ \text{min}^{-1}$

$K_e = 6.75\ \text{mole}/\ell,$

and experimentally measured single-solute adsorption data in Eq. (3) were used as input parameters.

The elution profiles of the product stream are plotted in Figs. 3-9 as a function of the angular position at the exit of the reactor. In Fig. 3 the prediction by the numerical simulation gives good agreement with experimental data. Figure 4 reports data for a feed stream consisting of an equilibrium mixture, and sampled by the rotating sampling method. The data points exhibit more scatter than those of Fig. 3, which we attribute to non-uniformity of bed packing. This is not a factor in the fixed-point sampling scheme. The data of Fig. 4 are fit quite well to the simulation results, both with respect to peak shapes and peak positions.

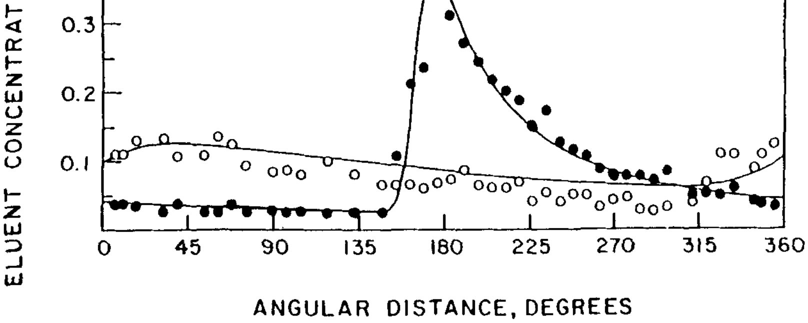

Figure 3 Adjusted elution profiles. ● methanol, ○ formic acid. - numerical simulation. See Table 1 for experimental conditions.

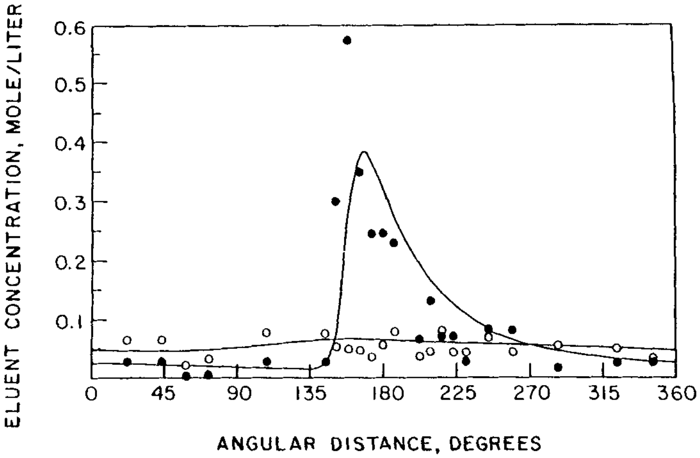

Figure 4 Elution profiles. ● methanol, ○ formic acid. - numerical simulation. See Table 1 for experimental conditions.

Figure 5 shows the elution profiles when the rotation speed of the feed port was reduced by one half, with other operating conditions remaining the same. The agreement between simulation results and experimental data are again quite good except for slight shifts of peak positions. The sharper peaks and the smaller elution angle in Fig. 5 than those in Fig. 3 are intuitively correct, for the slower rotation speed implies a larger amount of reactant feed per unit angle.

Figure 6 shows the elution profiles when the reaction rate was reduced by a factor of two, by reducing the catalyst concentration. The peak shapes of Fig. 6 are almost the same as those of Fig. 5, except their heights are slightly lower. The peak positions are also almost the same, which means that the reduced reaction rate is still fast enough to provide ample time for reaction as well as good separation. It is anticipated that at sufficiently slow rates there would be more peak overlap.

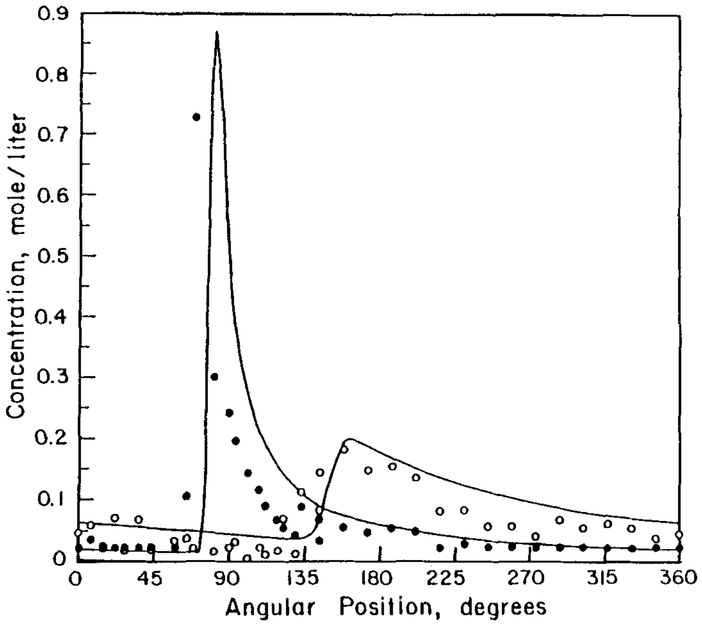

Figure 5 Elution profiles. ● methanol, ○ formic acid. – numerical simulation. See Table 1 for experimental conditions.

The reactor bed was left unwashed for about one month between the data taken in Figs. 6 and 7. It was then washed out, and Fig. 7 shows the results in which the feed concentration was reduced to 2 mole/ℓ. The methanol peak is fit very well, but the formic acid peak reveals large discrepancies with the model simulation results. This may be due to:

a) inadequate temperature control of the system,

b) improper washing of the reactor bed between experimental runs,

c) deactivation or impurity contamination of the adsorption sites for formic acid.

However, causes a) and b) may be dismissed because the temperature

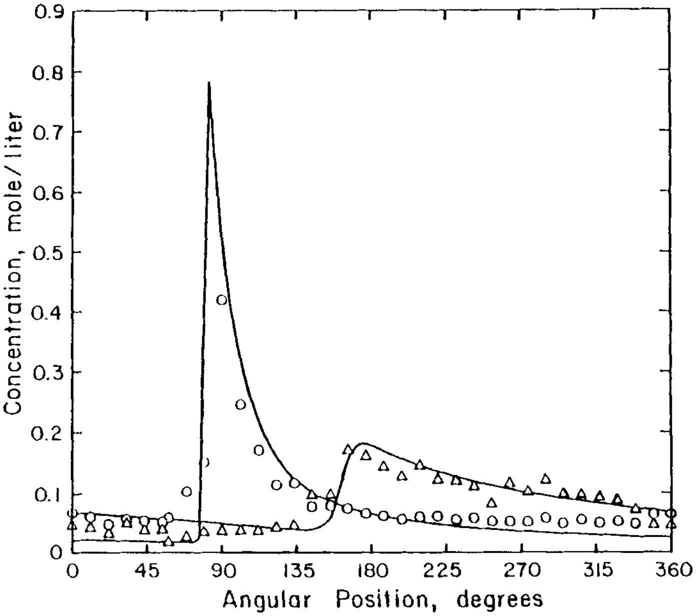

Figure 6 Elution profiles. ○ methanol, △ formic acid. - numerical simulation. See Table 1 for experimental conditions.

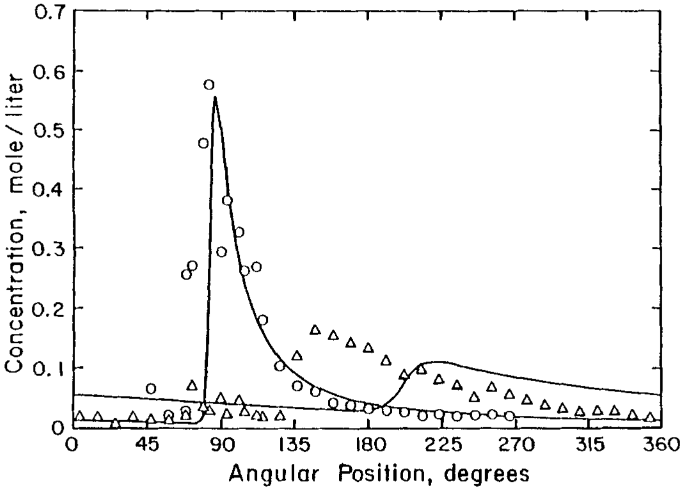

Figure 7 Elution profiles. ○ methanol, △ formic acid. - numerical simulation. See Table 1 for experimental conditions.

control and the washing process were always consistent. Therefore, it can be concluded that the adsorption sites for formic acid were deactivated or irreversibly contaminated with impurities, most probably due to the long contact with reaction mixture. The data in Fig. 8 were obtained with a feed concentration of 1.5 mole/ℓ, with special attention given to the temperature and the pre-washing of the bed. The results gave good agreement for the methanol peak, but the discrepancies in the formic acid profile still remained, thus reinformcing the deactivation hypothesis.

Finally, both the rotation speed of the feed port and the fluid flow velocity were reduced to half of those of Fig. 3. From the model, Eq. (4), we expect that this will have the same effect on the elution profiles as if the reaction rate were doubled. From results in Figs. 3 and 6, it was found that the change of the reaction rate in this range has little effect on the elution profile. Therefore, we expect the elution profiles, shown in Fig. 9, be very similar to those of Fig. 3. The experimental data again show excellent agreement for the methanol peak, but the formic acid peak has the same discrepancies as before.

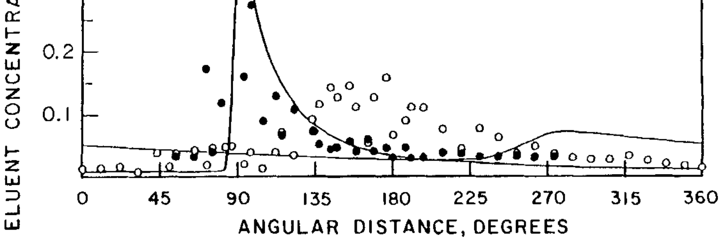

Figure 8 Elution profiles. ● methanol, ○ formic acid. – numerical simulation. See Table 1 for experimental conditions.

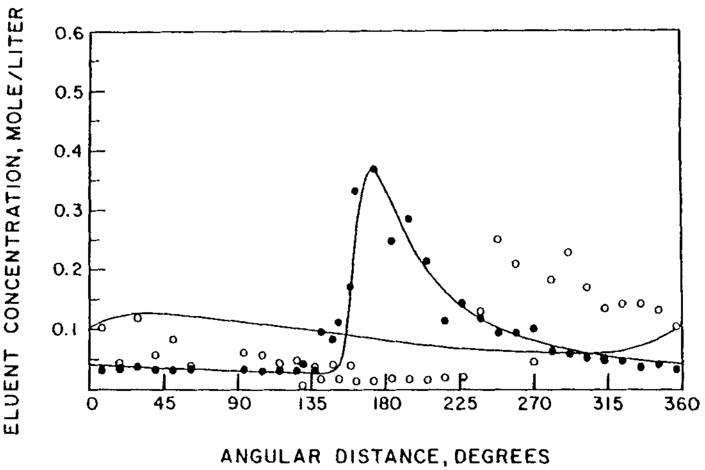

Figure 9 Elution profiles. ● methanol, ○ formic acid. - numerical simultiona. See Table 1 for experimental conditions.

It can be concluded that the activated coconut charcoal under the HCl environment deactivates slowly, first on adsorption sites for methanol, and then on those for a stronger adsorbate like formic acid and methylformate. For long term use of this continuous chromatographic reactor, therefore, this deactivation process should be thoroughly investigated.

Experimental and numerical simulation results on the overall conversion level are summarized in Table 2.

The differences revealed in Table 2 between experimental and numerical results are due to the fact that methylformate concentrations below 0.002 mole/ℓ (120 ppm) could not be effectively detected by the GC analysis used in this study.

CONCLUSIONS

A continuous annular chromatographic reactor was used for the aqueous, acid catalyzed hydrolysis of methylformate. The reaction products, methanol and formic acid, gave reasonably well defined

TABLE 2. Degree of Overall Conversion

Figure	Thermodynamic Conversion Limit	Simulation Results	Experimental Results
3	75.40%	98.85%	100.0%
4	0.0	98.76	100.0
5	75.44	98.99	100.0
6	75.44	96.93	100.0
7	81.08	99.34	100.0
8	84.57	99.47	100.0
9	75.44	98.84	100.0

chromatographic peaks. No reactant was detected in the effluent, indicating that the reaction went virtually to completion.

The adsorbent, activated coconut charcoal, appeared to deactivate after long use in the hydrochloric acid environment. The signs of deactivation for adsorption appeared first for methanol, which is the weakest adsorbate, and then for formic acid.

A simple mathematical model of this reactor was developed assuming isothermal and ideal chromatographic conditions, where effects of dispersion and nonequilibrium adsorption were presumed negligible. This ideal chromatographic model was simulated numerically, and proved to be capable of giving excellent prediction of experimental results.

The competitive multicomponent adsorption process of this reaction mixture is not completely understood. In the numerical simulation, the Freundlich adsorption isotherm was used, in which competitive adsorption was not considered. Even these single-solute adsorption isotherm data were sufficient to obtain a good prediction of the experimental results. This seems to be due to the quick disappearance of the high concentration of methylformate a short distance from the reactor inlet, and almost no competitive adsorption between methanol and formic acid.

It is evident that this type of continuous chromatographic reactor can be applied to reactions with highly unfavorable equilibrium conditions, though minor improvements in the apparatus remain to be made.

ACKNOWLEDGEMENT

This work was supported by the U.S. Department of Energy under contract No. EY-76-02-2945.

NOMENCLATURE

A	methylformate
B	methanol
c	fluid phase concentration, mole/ℓ
C	formic acid
k	forward reaction rate constant, $\min^{-1}$
K	adsorption equilibrium constant, mole/gr of adsorbent
K_e	reaction equilibrium constant, mole/ℓ
m	exponential factor in the Freundlich adsorption isotherm, $n_i = K_i c_i^{m_i}$
n	solid surface concentration, mole/gr of adsorbent
R	mean value of the reactor radius, $(R_1 + R_2)/2$
R_1	radius of the inner cylinder, cm
R_2	radius of the outer cylinder, cm
u	flow velocity of the fluid phase, cm/min
z	axial distance along the reactor, cm

Greek Symbols

ε	void fraction of the reactor bed
ρ_B	reactor bed density, gr of adsorbent/cc of bed
ϕ	angular distance, radian
Φ	angular width of the reactant feed port, 0.06π
ω	angular velocity of rotation of the feed port, rad/min

Subscripts

A	methylformate
B	methanol
C	formic acid
i	component A, B or C
o	inlet feed condition
z	axial component

REFERENCES

1. P. Antonucci and N. Giordano, J. Chromatog. 150, 309 (1978).

2. W. A. Blanton, C. H. Byers, and R. P. Merrill, I & EC Fundam. 7, 611 (1968).

3. G. A. Gaziev, V. Yu. Filinovskii, and M. I. Yanovskii, Kinet. i. Katal. 4, 688 (1963).

4. J. M. Matsen, J. W. Harding, and E. M. Magee, J. Phys. Chem. 69, 522 (1965).

5. S. Z. Roginskii, M. I. Yanovskii, and G. A. Gaziev, Kinet. i. Katal. 3, 529 (1962).

6. E. I. Semenenko, S. Z. Roginskii, and M. I. Yanovskii, Kinet. i Katal. 5, 490 (1964).

7. R. David and J. Villermaux, Can. J. Chem. Eng. 51, 630 (1973).

8. T. Hattori and Y. Murakami, Can. J. Chem. Eng. 52, 601 (1974).

9. P. A. Obraztsov and M. I. Vinnik, Kinet. i. Katal. 18(1), (Eng) 81 (1975).

10. M. I. Yanovskii and A. D. Berman, J. Chromatog. 69, 3 (1972).

11. A. J. P. Martin, Discussions Faraday Soc. 7, 332 (1949).

12. J. C. Giddings, Anal. Chem. 34, 37 (1962).

13. J. B. Fox, Jr., R. C. Calhoun, and W. J. Eglinton, J. Chromatog. 43, 48 (1969).

14. C. D. Scott, R. D. Spence, and W. G. Sisson, J. Chromatog. 126, 381 (1976).

15. P. C. Wankat, A. R. Middleton, and B. L. Hudson, I & EC Fundam. 15, 309 (1976).

16. M. V. Sussman, K. N. Astill, R. Rombach, A. Cerullo, and S. S. Chen, I & EC Fundam. 11, 182 (1972).

17. E. J. Tuthill, J. Chromatog. Sci. 8, 285 (1970).

18. P. E. Barker and D. Critcher, Chem. Eng. Sci. 13, 82 (1960).

19. S. Viswanathan and R. Aris, Adv. Chem. Ser. 133, 191 (1974).

20. B. K. Cho, R. W. Carr, and R. Aris, Proceedings, ISCRE 6, Pergamon Press (in press).

21. J. J. Kipling, Adsorption from Solutions of Non-electrolytes, Academic Press, New York, 1965.

22. P. D. Lax, Commun. Pure & Appl. Math. 7, 159 (1954).

23. J. H. Perry, Chemical Engineers' Handbook, 4th ed., McGraw-Hill, New York, 1963.

24. R. P. Bell, A. L. Dowding, and J. A. Noble, J. Chem. Soc. 3106 (1955).

25. R. G. Wetherold, E. H. Wissler, and K. B. Bischoff, Adv. Chem. Ser. 133, 181 (1974).